An Integrated Structures/Controls/Passive Damping Design Optimization Methodology

R. A. Manning
TRW Space and Technology Group

Introduction

The successful performance of many future space missions depends on new and innovative structural/control design techniques. It will also be necessary to exploit the synergistic design application of passive damping techniques to aid in eliminating harmful controls/structure interactions.

Recent work has successfully demonstrated the hardware implementation of viscoelastically damped passive members [1] and active members with embedded piezoelectric sensors and actuators [2,3]. The passive and active members suppress structural vibrations with minimal weight, complexity, and power consumption impact. Injecting these technologies early in the design process using an integrated design procedure, rather than a sequential design procedure, is the next step in their development and acceptance.

Bronowicki and Diaz presented analysis and optimization techniques for constrained layer, viscoelastically damped members in Ref. 1. The techniques were applied to a single member which was then successfully fabricated and tested. Design optimization techniques for viscoelastic damping treatments based on the modal strain energy method were presented in Ref. 4.

Regarding active members, a number of previous studies have demonstrated integrated structure/control design methods using member actuators. Lust and Schmit [5] examined an integrated optimization methodology for member actuators using direct output feedback. Thomas and Schmit [6] advanced this idea and added dynamic stability constraints to insure convergence to a stable design. McLaren and Slater [7] included various control compensators in their covariance approach to the integrated optimization problem. A useful finding of this latter work was the effect of the order of the compensator on the objective function (see Figures 4 and 8, Ref. 7).

The work presented herein is concerned with the development of an integrated design optimization methodology where structural, passive member, active member, and control compensator design variables are treated simultaneously. The integrated design process is intended for large complex structures where purely structural solutions or even sequential design solutions have little or no potential for success in meeting the stringent performance requirements. By including the compensator parameters in the optimization procedure, better performance can be obtained while meeting stability constraints than for direct output feedback.

System Description

Many future space systems will consist of baseline truss structures from which reflectors, antennae, communications equipment, and electronics equipment are mounted. For this reason, the work considered herein is concerned with truss structures augmented with passive and active members. It has been assumed that overall system performance can be derived from motions of specific points on the truss (e.g., the motions of mounting points for sensitive optical equipment).

The structural dynamic equations of motion can be written as

$$M\ddot{z} + [(1 + i\gamma^s)K^s + i\gamma^p K^p]z = P + bu \tag{1}$$

where M and K^s are the mass and stiffness matrices, z is the vector of displacements, and P is the vector of externally applied nodal loads. Inherent damping in the inert truss is modeled as structural damping and enters the equations through the γ^s parameter. The passive damping members contribute to the standard mass and stiffness matrices, but also add the damping term $i\gamma^p K^p$ [8]. Active members contribute to the standard mass and stiffness matrices, but also add the final term on the right hand side of equation (1). This final term consists of the b matrix locating actuators on the structure and the vector of actuation forces, u. Equation (1) can be written in the familiar state space form

$$\dot{X} = AX + Bu \tag{2}$$

Figure 1 shows the block diagram for such systems.

The plant consists of inert truss members, concentrated masses, viscoelastically damped members, and the unenergized active members. Sensor measurements are available and are given by

$$y = C_p X + D_p u \tag{3}$$

where the C_P matrix locates sensors on the structure. Closing the local loops around the active members activates the compensator (see Figure 1) which consists of the A_f, B_f, and C_f matrices. The specific elements of each of these matrices depend on the control law being used. For this work, a Positive Position Feedback (PPF) compensator [9] is tied around each active member.

The design variables and optimization variables for each type of element in the system are shown in Figure 2. For the inert truss members, the tube diameter and wall thickness were taken as design variables while the reciprocal of the cross sectional area was used as the optimization variables. For the passive members, the inside tube diameter and wall thickness, viscoelastic material thickness, and constraining layer thickness were the design variables. A mass penalty of 100% of the structural mass of the passive member was added to account for thermal control hardware. The optimization variables were chosen as the reciprocal of the areas of the inside tube, the viscoelastic material, and the constraining layer. For the active members, the inside dimension and wall thickness of the member were taken as design variables whereas the reciprocal of the area was used as the optimization variable. A mass penalty of 200% of the structural mass of the active member was added to account for thermal control, electronics, and power consumption hardware. Design and optimization variables for the local compensator wrapped around each active member were the filter frequency and damping ratio and the overall compensator gain.

Optimum Design Problem Statement

For many space missions, a single performance index, such as line-of-sight (LOS) or pointing error, is the critical parameter for mission success. Minimization of this quantity is the goal of the design process to maximize system performance. However, additional constraints must be imposed on other quantities within the system. For example, line-of-sight may depend on the relative displacement and rotation of a number of optical elements within the system. The goal of the optimization process is to minimize LOS without allowing any of the optical elements to exceed their range of motion or hit their mounting stops.

For such missions, the optimization problem can be stated as

$$\min \ \mathrm{LOS(d,f)} \tag{4}$$

subject to

$$g(d,f) \leq 0 \tag{5}$$

along with the side constraints

$$d^l \leq d \leq d^u \tag{6}$$

where it is understood that d is the vector of design variables for the inert truss members, passive damping members, and active members as discussed in the previous section.

In general, the design problem stated in equations (4) through (6) is an implicit nonlinear mathematical programming problem. Furthermore, embedded within the optimum design problem statement is the placement of the passive and active members on the structure. The placement aspect of the design problem requires a computationally burdensome combinatoric optimization solution technique. It can be stated from a computational experience viewpoint that the design problem posed in equations (4) through (6) defies attempts at a direct solution.

Solution Methodology

In this work, the solution procedure for the optimum design problem stated in equations (4) through (6) is broken into a heuristic subproblem and a formal subproblem. In the heuristic subproblem, locations for the passive and active members are determined by examining regions of high strain energy for those modes which contribute most to the objective function and the constraints. Once the locations of the passive and active members have been found, a formal subproblem based on equations (4) through (6) is solved. The formal subproblem replaces the implicit problem posed in equations (4) through (6) with the explicit approximate problem

$$\min \ \mathrm{L\tilde{O}S(d,f)} \tag{7}$$

subject to

$$\tilde{g}(d,f) \leq 0 \tag{8}$$

along with the side constraints

$$d^l \leq d \leq d^u \tag{9}$$

The $L\tilde{O}S$ and $\tilde{g}$ represent explicit first order Taylor series approximations for the objective function and constraints, respectively.

Solution of the implicit optimum design problem posed in equations (4) through (6) proceeds by solving a sequence of heuristic and formal subproblems. Each formal subproblem involves solving a sequence of approximate problems (stated in equations (7) through (9)). A pictorial description of the complete solution sequence to the original optimum design problem is shown in Figure 3.

Example Problem

In this section, the optimum design procedure described in the previous sections is demonstrated on an example problem. The example problem chosen is a potential concept for a Space Based Interferometer (SBI) [10] and is shown in Figure 4. The interferometer consists of an 11 meter tower with a telescope running down the center of it. Two 13 meter arms are attached at the base of the tower and support collecting telescopes at their tips. The 13 meter arms yield a baseline optical path length of 26 meters. Laser metrology equipment is mounted at the end of an 11 meter truss.

The performance of the SBI is maximized when optical path length excursions from 26 meters are minimized during expected on-orbit wideband disturbances. Thus the optimum design problem is to minimize optical path length excursions from 26 meters with upper bound constraints of 10 μradians and 5 μradians on the relative tilt and tip of the collecting telescopes, respectively. An upper bound cap on the total system weight is also imposed to insure that the SBI is within the launch vehicle's capability for a given orbit.

An initial structural design, which satisfies strength and geometric limitations imposed on the SBI, was used as the point of departure for the optimum design procedure. The initial design (see Table 1) has a mass of 252 kgs. The initial mass of 252 kgs serves as the upper bound weight cap as described above. Figure 5 shows the performance of the interferometer at the initial design. The modes at 4.4, 8.4, 19.1, 27.5, and 36.5 Hz contribute to unacceptable optical lengths as well as relative tilt and tip motions of the collecting telescopes exceeding their bounds.

The heuristic subproblem for active and passive member locations was solved by placing these members in regions of high strain energy for the troublesome modes. Optimum values for the design variables were found by solving the formal subproblem. Four to five approximate problem solutions were typically needed to achieve acceptable designs.

Table 1 contains the initial and final designs as well as the values of the objective function and constraints. Nine active members and four passive members with a total mass of 11 kgs were utilized in achieving these results. The performance of the interferometer at the optimum design is shown in the bottom trace in Figure 5. The integrated design optimization methodology achieved a factor of 38 improvement in SBI baseline while regaining feasibility with respect to telescope tilt and tip responses.

Concluding Remarks

An integrated structures/passive damping/active controls design optimization methodology has been described. The design optimization methodology avoids the combinatoric nature of active/passive member placement by splitting the solution procedure into a heuristic subproblem and a formal subproblem. During the heuristic subproblem, efficient locations for the damping devices are chosen, whereas during the formal subproblem, design sensitivity information and approximation concepts are employed to size the design variables.

The integrated nature of the design process takes advantage of the synergy that exists between the disciplines. By designing damping into the system early in the design process, superior performance can be achieved when compared to retrofit damping and/or purely structural solutions.

Simultaneous design of the compensator for the active members allows damping to be designed into the system without destabilizing the higher modes.

References

[1] Bronowicki, A.J. and Diaz, H.P., "Analysis, Optimization, Fabrication and Test of Composite Shells with Embedded Viscoelastic Layers", Presented at Damping '89, West Palm Beach, Florida, February 8-10, 1989.

[2] Bronowicki, A.J., Manning, R.A., and Mendenhall, T.L., "TRW's Approach to Intelligent Space Structures", presented at the ASME Winter Annual Meeting, San Fransisco, California, December 13-15, 1989.

[3] Fanson, J.L., Blackwood, G.H., and Chu, C-C., "Active-Member Control of Precision Structures", *Proceedings of the AIAA/ASME/ASCE/AHS/ASC 30th Structures, Structural Dynamics, and Materials Conference*, Mobile, Alabama, April 3-5, 1989, pp. 1480-1494.

[4] Gibson, W.C¿ and Johnson, C.D., "Optimized Designs of Viscoelastic Damping Treatments", *Damping 89 Proceedings*, Air Force Wright Aeronauitcal Laboratories, Report AFWAL-TR-89-3116, Vol. 1, February 1989.

[5] Lust, R.V. and Schmit, L.A., "Control-Augmented Structural Synthesis", *AIAA Journal*, Vol. 26, Jan. 1988, pp. 86-94.

[6] Thomas, H.L. and Schmit, L.A., "Control Augmented Structural Synthesis with Dynamic Stability Constraints", *Proceedings of the AIAA/ASME/ASCE/AHS/ASC 30th Structures, Structural Dynamics, and Materials Conference*, Mobile, Alabama, April 3-5, 1989, pp. 521-531.

[7] McLaren, M.D. and Slater, G.L., "A Covariance Approach to Integrated Control/Structure Optimization", *Proceedings of the 31st AIAA Dynamics Specialists Conference*, Long Beach, California, April 5-6, 1990, pp. 189-205.

[8] Hedgepeth, J.M. and Mobren, M., "Investigation of Passive Damping of Large Space Truss Structures", *Damping 86 Proceedings*, Air Force Wright Aeronauitcal Laboratories, Report AFWAL-TR-86-3059, Vol. 1, May 1986.

[9] Fanson, J.L. and Caughey, T.K., "Positive Position Feedback Control for Large Space Structures", *Proceedings of the 28th AIAA Dynamics Specialists Conference*, Monterey, California, April 9-10, 1987, pp. 588-598.

[10] Laskin, R.A., "A Spaceborne Optical Interferometer: The JPL CSI Mission Focus", *Proceedings of the NASA/DoD Controls-Structures Interaction Technology Conference*, NASA CP 3041, San Diego, California, January 29-February 2, 1989, PP. 1-16.

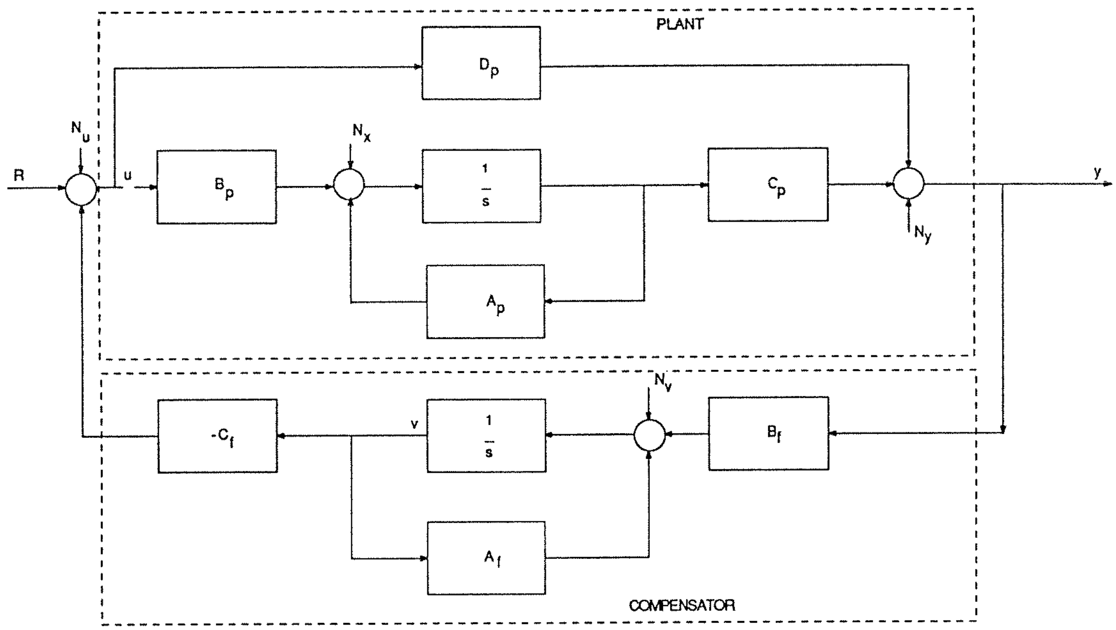

Figure 1: System Block Diagram

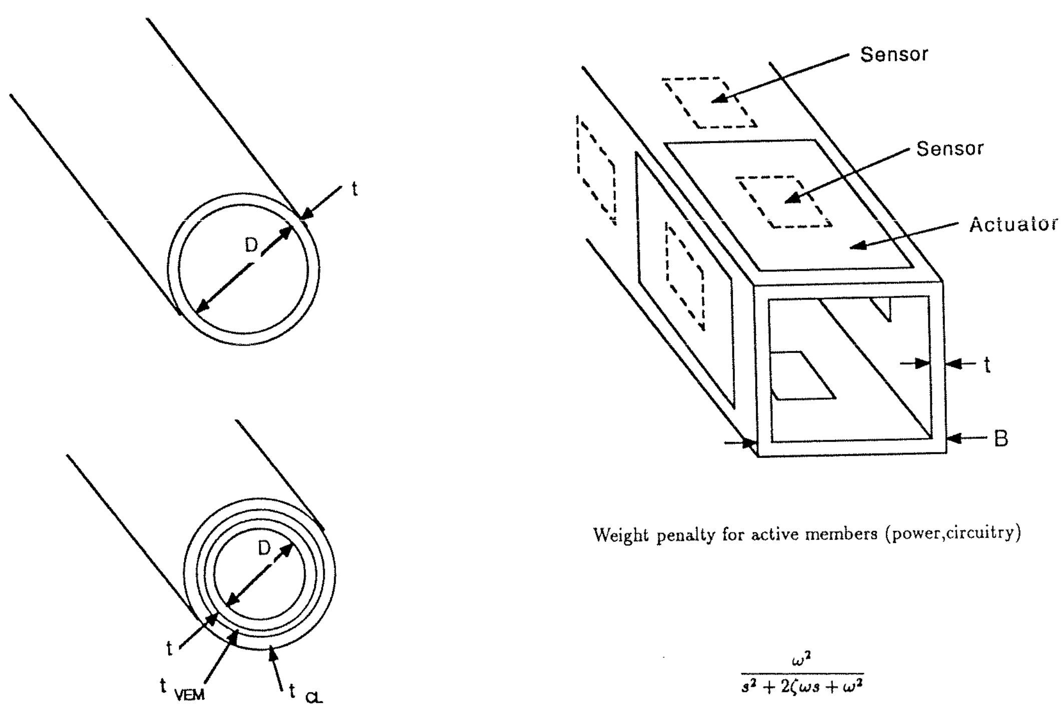

Weight penalty for passive members (thermal control)

Weight penalty for active members (power,circuitry)

$$\frac{\omega^2}{s^2 + 2\zeta\omega s + \omega^2}$$

PPF doesn't require zero knowledge

Figure 2: Design Element Details

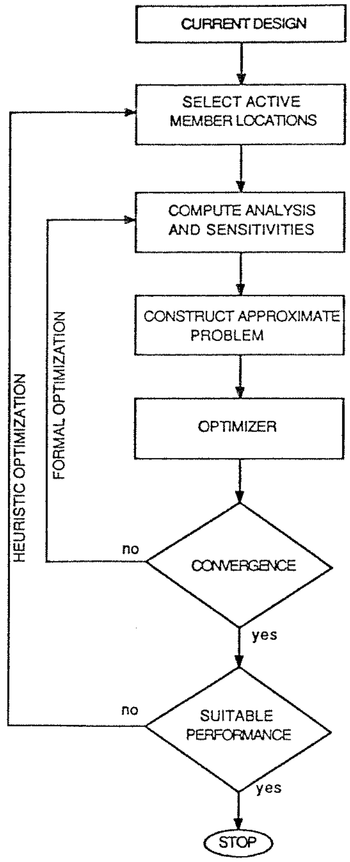

Figure 3: Solution Procedure Flow Diagram

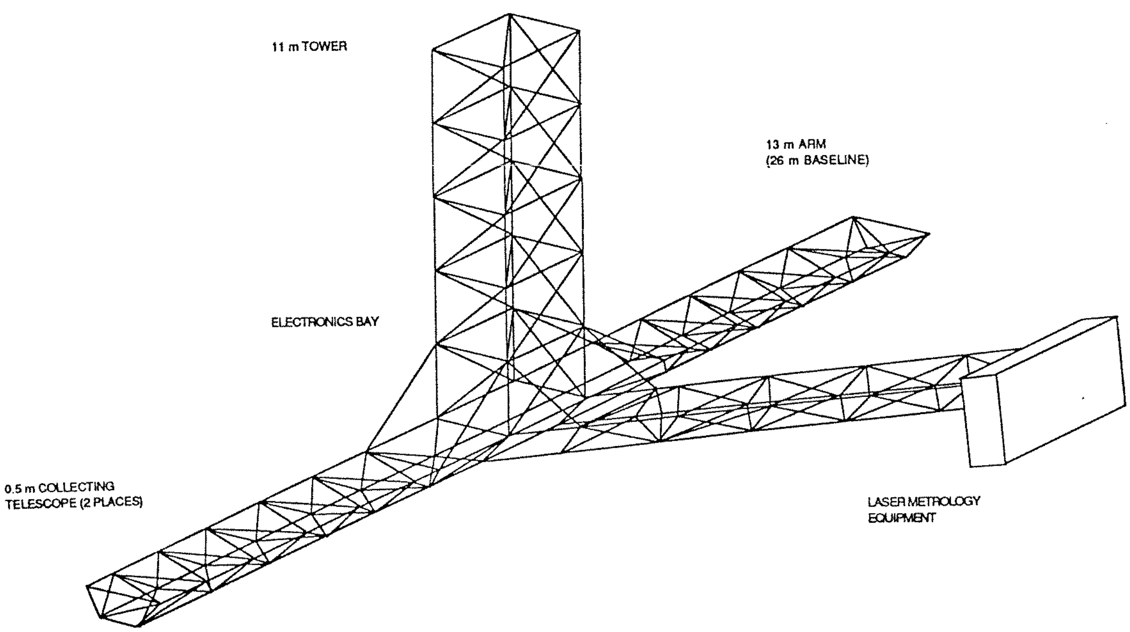

Figure 4: Space Based Interferometer Concept

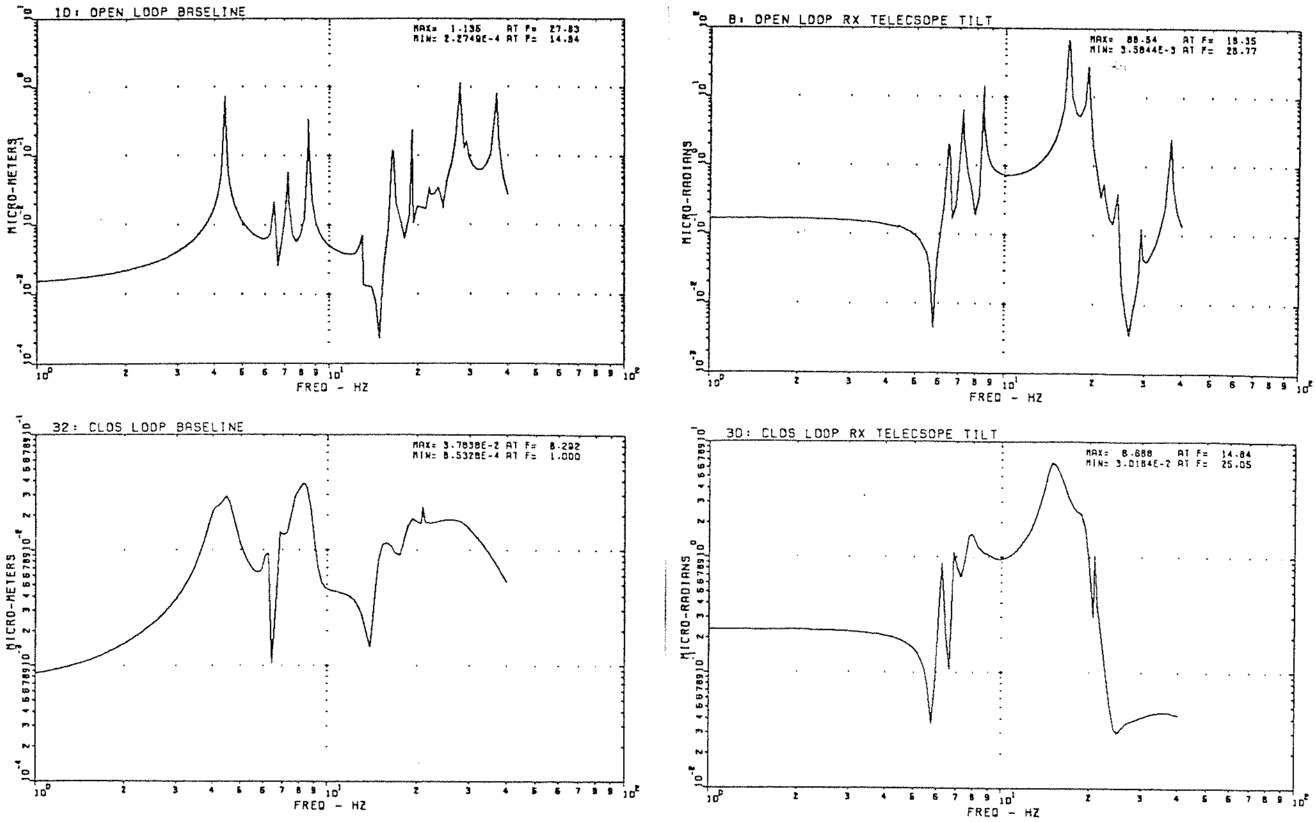

Figure 5: Initial and Final Baseline Response

Table 1: Initial and Final Designs

Description	Initial Values	Final Values
Longerons	25.4 mm D, 1.5 mm t	25.4 mm D, 1.4 mm t
Side and Top Diagonals	25.4 mm D, 1.5 mm t	25.4 mm D, 1.2 mm t
In-Plane Diagonals	12.7 mm D, 0.8 mm t	12.7 mm D, 0.8 mm t
Tower Longerons	25.4 mm D, 1.5 mm t	25.4 mm D, 1.4 mm t
Metrology Longerons	25.4 mm D, 1.5 mm t	25.4 mm D, 1.4 mm t
Passive Members	-	25.4 mm D, 1.3 mm t
VEM Thickness	-	0.2 mm
Constraining Layer Thickness	-	0.1 mm
Active Members	-	25.4 mm B, 1.3 mm t
Compensator Frequencies (Hz)	-	8.2,4.3,15.4,
	-	15.4,17.8,8.3
Compensator Damping	-	0.10,0.10,0.10,
	-	0.15,0.10,0.10
System Mass (kg)	252	252
Baseline (μm)	1.14	0.03
Telsecope Tilt (μrad)	68.54	6.67
Telescope Tip (μrad)	32.64	3.63